PCCP

Isotherm Model for Moisture-Controlled CO_2 Sorption

Journal:	*Physical Chemistry Chemical Physics*
Manuscript ID	CP-ART-03-2022-001131.R1
Article Type:	Paper
Date Submitted by the Author:	04-May-2022
Complete List of Authors:	Kaneko, Yuta; Arizona State University, School of Sustainable Engineering and the Built Environment Lackner, Klaus; Arizona State University, School of Sustainable Engineering and the Built Environment

PCCP

ARTICLE TYPE

Cite this: DOI: 00.0000/xxxxxxxxxx

Received Date
Accepted Date

DOI: 00.0000/xxxxxxxxxx

Isotherm Model for Moisture-Controlled CO_2 Sorption[†]

Yuta Kaneko[a] and Klaus S. Lackner[a]

Moisture-controlled sorption of CO_2, the basis for moisture-swing CO_2 capture from air, is a novel phenomenon observed in strong-base anion exchange materials. Prior research has shown that Langmuir isotherms provide an approximate fit to moisture-controlled CO_2 sorption isotherm data. However, this fit still lacks a governing equation derived from an analytic model. In this paper, we derive an analytic form for an isotherm equation from a bottom-up approach, starting with a fundamental theory for an alkali liquid. In the range of interest relevant to CO_2 capture from air, an isotherm equation for an alkali liquid reduces to a simple analytic form with a single parameter, K_{eq}. In the limit $K_{\text{eq}} \gg 1$, a 2nd order approximation simplifies to a Langmuir isotherm that, however, deviates from experimental data. The isotherm theory for an alkali liquid has been generalized to a strong-base anion exchange material. In a strong-base anion exchange material, water concentration inside a sorbent, $[\mathrm{H_2O}]$, is not large enough to be regarded as constant, which allows us to extend K_{eq} to $K_{\text{eq(AEM)eff}} = K_{\text{eq(AEM)}} \times [\mathrm{H_2O}]^{-n}$ according to the law of mass action. The final isotherm formula has been validated by experimental data from the literature. For a moisture-controlled CO_2 sorbent, $K_{\text{eq(AEM)eff}}$ varies significantly with moisture content of the sorbent. Depending on moisture level, the observed $K_{\text{eq(AEM)eff}}$ in a specific sorbent ranges from a few times to a few thousand times the value of K_{eq} of a $2\,\mathrm{mol\,L^{-1}}$ alkali liquid.

1 Introduction

Moisture-controlled CO_2 sorption[1 2] is a novel phenomenon observed in strong-base anion exchange materials (AEMs) with quaternary ammonium cations. The CO_2 equilibrium partial pressure over these sorbents can increase roughly 500-fold as the relative humidity is raised from 20% to 100%[3 4]. This makes it possible to develop a cycle of sorption and desorption that is driven by moisture rather than a direct energy input, i.e., a moisture-swing sorbent cycle and its application to CO_2 capture from ambient air (Direct Air Capture, DAC). DAC has been introduced to balance the carbon budget[5 6 7]. It is useful in capturing CO_2 from fossil carbon emissions that could not be collected at large point sources, or has been generated at myriad small and distributed sources like automobiles, trucks, ships and airplanes. In more recent years the emphasis has shifted to negative emissions that are necessary to draw down excess carbon from the environment[8 9]. DAC is one of the Negative Emission Technologies (NETs)[10] that are necessary to limit global warming to 1.5°C[11 12 13], however, the high energy demand and cost are currently the most challenging issues for DAC applications[14 15 16]. Since water is a cheaper resource compared to the heat that is necessary for temperature-swing-based DAC[17 18], moisture-controlled CO_2 sorption may reduce the cost of DAC.

In general, many different types of empirical formulas have been proposed to fit various isotherm data[19]. Langmuir isotherms offer an approximate fit to moisture-controlled CO_2 sorption isotherm data[3 4 20], but this approximation is not grounded in an analytic model and its governing equations. Such a model is critical to understanding the thermodynamics of this novel sorption mechanism. To characterize sorbents in more a quantitative way, we investigated the analytic CO_2 isotherm equation that can be directly derived from the governing equations of moisture-controlled CO_2 sorption.

There is good evidence that the reaction of CO_2 binding to AEMs that exhibit moisture-controlled sorption is analogous to the sorption of CO_2 into alkaline aqueous solutions. Because of their high ionic charge density these AEMs always contain water embedded into the polymer matrix. The mobil anionic charge is embedded into this water, while the cationic charge in the form of quaternary ammonium ions is firmly affixed to the polymer matrix. The AEM can be considered as an aqueous solution of anions

---

[a] School of Sustainable Engineering & the Built Environment, Arizona State University, Tempe, AZ 85287, United States. Tel: 480-727-2499; E-mail: Klaus.Lackner@asu.edu

† Electronic Supplementary Information (ESI) available: Derivation of the approximate isotherm equation for negligible $[\mathrm{CO_2}]$ and $[\mathrm{H^+}]$ (S_{III}); derivation of the approximate isotherm equation for negligible $[\mathrm{CO_2}]$, $[\mathrm{H^+}]$ and $[\mathrm{OH^-}]$ (S_{IV}); and derivation of the Langmuir approximation of the isotherm (S_{V}).

perturbed by a polymer matrix to which the cations are attached. This description is supported by various numerical simulations on the atomistic level that indeed reproduce the moisture-swing effect[21 22 23].

In developing a continuum model we therefore start from a description which is very similar to that used to describe an aqueous solution of an alkali cations but assumes that the modification of the property of water inside the strong-base AEM makes different equilibrium constants. This model is very different from those derived by treating CO_2 binding as a surface adsorption effect, i.e., a surface complexation model[24], such as Van Cappellen's model[25]. In AEMs the CO_2 binding happens throughout the volume of the sorbent material. This is supported by experimental evidence. For example, Tao Wang's early capacity measurements show that the CO_2 loading can reach every charge site inside a strong-base AEM[3 4]. Even though the water-mineral interaction on mineral surfaces may have some similarities to the carbonate-bicarbonate chemistry inside a strong-base AEM, the chemistry in the interior of the strong-base AEM cannot be controlled by a surface potential. Therefore, the governing equations of Van Cappellen's model do not apply to our case. Van Cappellen's model requires a surface charge layer. Strong-base AEMs, which are not limited to membrane geometry with a high surface-to-volume ratio but also include amorphous spherical beads at the millimeter scale, must obey charge neutrality.

While moisture-controlled CO_2 sorption is a novel phenomenon and the interactions among CO_2, H_2O and the strong-base AEM are not fully understood yet, research regarding CO_2 absorption in alkali liquids has a very long history of nearly a hundred years[26] and it has been widely investigated because it is of theoretical interest and industrial importance[27 28 29 30]. Most importantly, the values of key parameters such as the equilibrium constants of the chemical reactions are reported in the literature[31 32 33 34], which is vital to understand the nature of CO_2-H_2O-alkali liquid interactions. The magnitude of chemical equilibrium constants varies dramatically with concentrations, temperatures and chemical composition, which greatly affects the behavior. In this paper, we initially establish CO_2 sorption isotherm equations for an alkali liquid optimized in our Area of Interest, where the partial pressure of CO_2 is within the range relevant to CO_2 capture from air, a few tens of Pascal for absorption and up to more than 10 kPa for desorption. Then, we extend the theory from alkali liquids to strong-base AEMs to derive an analytic expression of the moisture-controlled CO_2 sorption isotherm equation.

2 Chemisorption isotherms for alkali liquids and strong-base AEMs

2.1 Exact isotherm equation for alkali liquids

We start with an alkali liquid in equilibrium with CO_2 that results in a bicarbonate-carbonate-hydroxide system. Examples include a potassium bicarbonate aqueous solution or a sodium carbonate aqueous solution. We define alkalinity of an alkali liquid as concentration of positive charges excluding H^+ minus negative charges excluding OH^-, HCO_3^-, and CO_3^{2-} [27]. The alkalinity is denoted by [A]. Charge neutrality demands:

$$[A] + [H^+] = [HCO_3^-] + 2[CO_3^{2-}] + [OH^-] \tag{1}$$

where, $[i]$ denotes the concentration of the chemical species i. If other ions, e.g., chlorides are present, the alkalinity would include them and include all charges except for protons, hydroxides, carbonates and bicarbonates. Note that HCO_3^-, CO_3^{2-} and OH^- can also be regarded as the counter ions in case of strong-base AEMs that has been exchanged into the hydroxide form and then equilibrated against a certain partial pressure of CO_2. The following four equations apply simultaneously[28 29 30]:

$$CO_{2\,(g)} \xrightleftharpoons{K_H} CO_{2\,(aq)} \tag{2}$$

$$CO_{2\,(aq)} + OH^- \xrightleftharpoons{K_1} HCO_3{}^- \tag{3}$$

$$HCO_3{}^- + OH^- \xrightleftharpoons{K_2} CO_3{}^{2-} + H_2O \tag{4}$$

$$H_2O \xrightleftharpoons{K_W} H^+ + OH^- \tag{5}$$

Note that the subscript g and aq refer to the gaseous and dissolved phase, respectively. We assume that these equations hold both for an aqueous solution and an AEM. However, the equilibrium constants can be different.

By eliminating the $[OH^-]$ term, we obtain[28 29]:

$$2\,HCO_3{}^- \rightleftharpoons CO_3{}^{2-} + CO_{2\,(aq)} + H_2O \tag{6}$$

Note that the first reaction happens only at the surface of an aqueous solution since CO_2 in gaseous phase exists only outside the solution. For a system in chemical equilibrium, Henry's constant and the equilibrium constants of each chemical reaction are defined as:

$$K_W \equiv [H^+][OH^-] \tag{7}$$

$$K_H \equiv \frac{[CO_2]}{P_{CO_2}} \tag{8}$$

$$K_1 \equiv \frac{[HCO_3^-]}{[CO_2][OH^-]} \tag{9}$$

$$K_2 \equiv \frac{[CO_3^{2-}]}{[HCO_3^-][OH^-]} \tag{10}$$

where P_{CO_2} denotes the partial pressure of the gaseous CO_2. Henry's law is valid since P_{CO_2} is much smaller than 1 atm in our Area of Interest. Note that $[CO_2]$ represents the concentration of CO_2 inside the aqueous solution, not that in the gas phase outside. Also note that we follow the convention that $[CO_2]$ also includes the small additional contribution of $[H_2CO_3]$. To understand orders of magnitude and to introduce a reference value, we define K_W°, K_H°, K_1° and K_2° as the value of these equilibrium constants for an ideal solution at 25°C. The literature[34] indicates:

$$K_W^\circ = 1.0 \times 10^{-14} \quad [\mathrm{mol^2\,L^{-2}}] \tag{11}$$
$$K_H^\circ = 3.3 \times 10^{-7} \quad [\mathrm{mol\,L^{-1}\,Pa^{-1}}] \tag{12}$$
$$K_1^\circ = 4.4 \times 10^{7} \quad [\mathrm{mol^{-1}\,L}] \tag{13}$$
$$K_2^\circ = 4.6 \times 10^{3} \quad [\mathrm{mol^{-1}\,L}] \tag{14}$$

Substituting Eq.(7), Eq.(9) and Eq.(10) into Eq.(1) yields:

$$[\mathrm{OH^-}] = [\mathrm{A}] + K_W/[\mathrm{OH^-}] - K_1[\mathrm{CO_2}]\left\{[\mathrm{OH^-}](1+2K_2[\mathrm{OH^-}])\right\} \tag{15}$$

Therefore, $[\mathrm{CO_2}]$ can be expressed as a function of $[\mathrm{OH^-}]$:

$$[\mathrm{CO_2}] = \frac{-[\mathrm{OH^-}]^2 + [\mathrm{A}][\mathrm{OH^-}] + K_W}{K_1[\mathrm{OH^-}]^2 + 2K_1K_2[\mathrm{OH^-}]^3} \tag{16}$$
$$\equiv f([\mathrm{OH^-}]) \tag{17}$$

Conversely, we can implicitly express $[\mathrm{OH^-}]$ as a function of $[\mathrm{CO_2}]$:

$$[\mathrm{OH^-}] = f^{-1}([\mathrm{CO_2}]) \tag{18}$$

A useful concept to simplify the equations is the Dissolved Inorganic Carbon (DIC), which is defined as

$$[\mathrm{DIC}] \equiv [\mathrm{HCO_3^-}] + [\mathrm{CO_3^{2-}}] + [\mathrm{CO_2}] \tag{19}$$

We can express [DIC] as a function of only $[\mathrm{CO_2}]$ by substituting Eq.(9), Eq.(10) and Eq.(18) into Eq.(19) as

$$[\mathrm{DIC}] = K_1[\mathrm{CO_2}][\mathrm{OH^-}]\left(1+K_2[\mathrm{OH^-}]\right) + [\mathrm{CO_2}] \tag{20}$$
$$= [\mathrm{CO_2}]\left\{K_1 f^{-1}([\mathrm{CO_2}])\left(1+K_2 f^{-1}([\mathrm{CO_2}])\right)+1\right\} \tag{21}$$

Next, we define θ as a ratio of absorbed carbon to alkalinity:

$$\theta \equiv [\mathrm{DIC}]/[\mathrm{A}] \tag{22}$$
$$= \frac{[\mathrm{CO_2}]\left\{K_1 f^{-1}([\mathrm{CO_2}])\left(1+K_2 f^{-1}([\mathrm{CO_2}])\right)+1\right\}}{[\mathrm{A}]} \tag{23}$$

Eq. (23) expresses the sorbent saturation as function of $[\mathrm{CO_2}]$ on the sorbent. As long as Henry's law applies, we can translate the latter into a corresponding equilibrium partial pressure of $\mathrm{CO_2}$ over the sorbent, i.e., the isotherm of this sorption/desorption reaction:

$$\theta = \frac{K_H P_{\mathrm{CO_2}}\left\{K_1 f^{-1}(K_H P_{\mathrm{CO_2}})\left(1+K_2 f^{-1}(K_H P_{\mathrm{CO_2}})\right)+1\right\}}{[\mathrm{A}]} \tag{24}$$

We refer to the exact isotherm (Eq.(24)) as $\theta = S_{\mathrm{I}}(P_{\mathrm{CO_2}})$. Fig.(1) and Fig.(2) show S_{I} plotted against $P_{\mathrm{CO_2}}$, $\mathrm{CO_2}$ concentration in 1-atm air in ppm, $[\mathrm{CO_2}]$ and pH, assuming [A] and temperature are respectively 2 $\mathrm{mol\,L^{-1}}$ and 25°C. $\theta = 0$, 0.5 and 1.0 in Fig.(1) means that $\mathrm{OH^-}$, $\mathrm{CO_3^{2-}}$ and $\mathrm{HCO_3^-}$ are respectively dominant over the others. The value at the x-intercept in Fig.(2) confirms that the pH of a 2 $\mathrm{mol\,L^{-1}}$ potassium or sodium hydroxide solution is 14.3. The pH at $\theta = 0.5$ in Fig.(2) is 12.2, corresponding to a potassium or sodium carbonate solution. At the bicarbonate point, $\theta = 1$, Fig.(2) confirms that the pH of a potassium or sodium bicarbonate solution is 8.3. When $[\mathrm{CO_2}]$ is very large, it is observed that θ goes beyond 1. $\mathrm{CO_2}$ loading exceeds the alkalinity due to the addition of carbonic acid to the solution. In this regime, the contribution of neutral $\mathrm{CO_2}$ is significant. However, our interest is focused on the range $0.5 < \theta < 1$.

2.2 Isotherm approximation for negligible concentrations of $[\mathrm{CO_2}]$

When $[\mathrm{CO_2}]$ is negligible compared to $[\mathrm{HCO_3^-}]$ or $[\mathrm{CO_3^{2-}}]$, we can approximate θ as:

$$\theta \sim \left\{[\mathrm{HCO_3^-}] + [\mathrm{CO_3^{2-}}]\right\}/[\mathrm{A}] \tag{25}$$
$$= K_H P_{\mathrm{CO_2}}\left\{K_1 f^{-1}(K_H P_{\mathrm{CO_2}})\left(1+K_2 f^{-1}(K_H P_{\mathrm{CO_2}})\right)\right\}/[\mathrm{A}] \tag{26}$$

We refer to this approximate isotherm (Eq.(26)) as $\theta = S_{\mathrm{II}}(P_{\mathrm{CO_2}})$. Fig.(1) and Fig.(2) confirm that this approximate solution is virtually identical to the exact solution in our Area of Interest ($0.5 < \theta < 1$) as long as θ is not very close to 1.

2.3 Isotherm approximation for negligible concentrations of $[\mathrm{CO_2}]$ and $[\mathrm{H^+}]$

When $[\mathrm{H^+}]$ is also negligible, we can express θ as an explicit function of $[\mathrm{CO_2}]$. Eq.(15) simplifies to:

$$[\mathrm{OH^-}] \sim [\mathrm{A}] - K_1[\mathrm{CO_2}]\left\{[\mathrm{OH^-}](1+2K_2[\mathrm{OH^-}])\right\} \tag{27}$$

This is a quadratic equation for $[\mathrm{OH^-}]$. By contrast, Eq.(15) is a cubic equation. We can solve this quadratic equation for $[\mathrm{OH^-}]$ and substitute the solution into Eq.(20) and Eq.(25). After some rearrangement of terms (see the Supplementary Information), we obtain the isotherm:

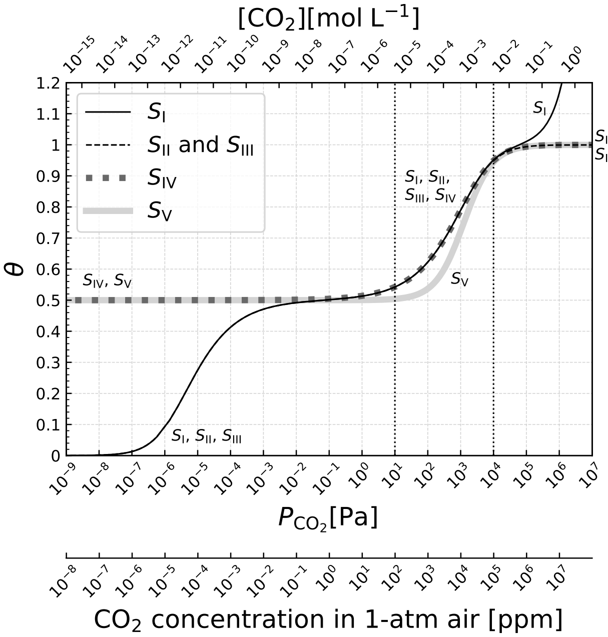

Fig. 1 The comparison of five expressions of θ as a function of $[\mathrm{CO_2}]$, $P_{\mathrm{CO_2}}$ or $\mathrm{CO_2}$ concentration in the gaseous phase in 1-atm air. [A] and temperature are respectively assumed to be 2 mol L^{-1} and 25°C. Note that all the x-axises use logarithmic scales. The vertical lines indicate the range of our Area of Interest.

$$\theta \sim (K_H K_1 P_{\mathrm{CO_2}} - 1) \times \frac{\sqrt{(1+K_H K_1 P_{\mathrm{CO_2}})^2 + 8K_H K_1 K_2 P_{\mathrm{CO_2}}[\mathrm{A}]} - (1+K_H K_1 P_{\mathrm{CO_2}})}{8K_H K_1 K_2 P_{\mathrm{CO_2}}[\mathrm{A}]} + \frac{1}{2} \tag{28}$$

We refer to this approximate isotherm (Eq.(28)) as $\theta = S_{\mathrm{III}}(P_{\mathrm{CO_2}})$. Fig.(1) and Fig.(2) confirm that this approximate solution is virtually identical to the exact solution in our Area of Interest ($0.5 < \theta < 1$). The difference between S_{II} and S_{III} appears only when $[\mathrm{H^+}]$ is close to or exceeds [A].

2.4 Isotherm approximation for negligible concentrations of $[\mathrm{CO_2}]$, $[\mathrm{H^+}]$ and $[\mathrm{OH^-}]$

When $K_H K_1 P_{\mathrm{CO_2}} (= [\mathrm{HCO_3^-}]/[\mathrm{OH^-}]) \gg 1$ is satisfied (negligible $[\mathrm{OH^-}]$ approximation), some rearrangement of terms in Eq.(28) (see the Supplementary Information) yields

$$\theta \sim \frac{K_{\mathrm{eq}} P_{\mathrm{CO_2}}}{4} \left(\sqrt{1 + \frac{4}{K_{\mathrm{eq}} P_{\mathrm{CO_2}}}} - 1 \right) + \frac{1}{2} \tag{29}$$

where,

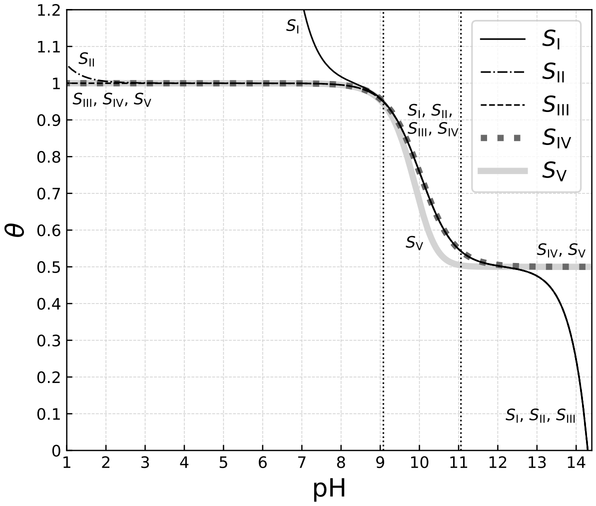

Fig. 2 The comparison of five expressions of θ as a function of pH. [A] and temperature are respectively assumed to be 2 mol L^{-1} and 25°C. The vertical lines indicate the range of our Area of Interest.

$$K_{\mathrm{eq}} \equiv \frac{K_1 K_H}{2K_2[\mathrm{A}]} \tag{30}$$

Note that the dimension of K_{eq} is an inverse pressure. We can define K_{eq}° for reference, which is the value of K_{eq} for an alkali liquid at 25°C that has $[\mathrm{A}] = 2\ \mathrm{mol\ L^{-1}}$. Substituting Eq.(12), Eq.(13) and Eq.(14) into Eq.(30) results in:

$$K_{\mathrm{eq}}^{\circ} = 7.9 \times 10^{-4} \quad [1/\mathrm{Pa}] \tag{31}$$

We refer to this approximate isotherm (Eq.(29)) as $\theta = S_{\mathrm{IV}}(P_{\mathrm{CO_2}})$. The graphs of S_{I} through S_{IV} are overlaid on top of each other in Fig.(1) and Fig.(2), using $K_{\mathrm{eq}} = K_{\mathrm{eq}}^{\circ}$. While S_{III} (Eq.(28)) can be explicitly expressed as a function of $P_{\mathrm{CO_2}}$ but has many material-specific independent parameters such as K_1, K_2 and [A], S_{IV} (Eq.(29)) contains only one parameter K_{eq} and is much easier to analytically handle compared to S_{I}, S_{II} and S_{III}. Nevertheless, S_{IV} is virtually identical to S_{I} in our Area of Interest, from a few tens of Pascal up to more than 10 kPa, according to Fig.(1) and Fig.(2).

2.5 The Langmuir approximation of the Isotherm

The Langmuir isotherm equation describes a system with a fixed number of binding sites that are all equivalent. For $\mathrm{CO_2}$ that is absorbed into an alkali solution, this is not quite a case. Instead, the binding is governed by the mass action laws (Eq.(2) through Eq.(5)). However, in the limit of a very large K_{eq}, the isotherm reduces to a Langmuir form. In this limit, one can assume $\frac{4}{K_{\mathrm{eq}} P_{\mathrm{CO_2}}} \ll 1$. A Taylor expansion of Eq.(29) up to the 2nd order term and some rearrangement of terms (see the Supplementary Information) yield

$$\theta \sim \frac{1}{2}\cdot\left(\frac{K_{\mathrm{eq}}P_{\mathrm{CO_2}}}{1+K_{\mathrm{eq}}P_{\mathrm{CO_2}}}\right)+\frac{1}{2} \tag{32}$$

This result means that the isotherm converges to a Langmuir isotherm defined between $0.5 < \theta < 1$ if $K_H K_1 P_{\mathrm{CO_2}} \gg 1$ and $K_{\mathrm{eq}}P_{\mathrm{CO_2}} \gg 1$ are satisfied. In other words, in this limit loading the solution from the carbonate state to the bicarbonate state follows an approximate Langmuir isotherm. Also, it has been explicitly demonstrated that K_{eq} has a physical meaning as Langmuir constant in this limit.

We refer to this approximate isotherm (Eq.(32)) as $\theta = S_{\mathrm{V}}(P_{\mathrm{CO_2}})$. Fig.(1) and Fig.(2) compare the Langmuir approximation with the other approximations. Here we can observe an obvious misfit between S_{I} and S_{V} even within our Area of Interest, especially at the lower $P_{\mathrm{CO_2}}$ around the ambient CO_2 level in the atmosphere ($\sim$ 400ppm). In this regime of our Area of Interest, the assumption of $K_{\mathrm{eq}}P_{\mathrm{CO_2}} \gg 1$ is not valid.

2.6 Generalization of the isotherm equations to strong-base AEMs

The above theory can be generalized to solid moisture-controlled CO_2 sorbents such as strong-base AEMs. This is possible, because the chemical reactions occurring inside the AEM are the same as in the aqueous solution (Eq.(2) through Eq.(5))[35 36]. However, the equilibrium constants will likely differ from those observed in aqueous solutions. The alkalinity of a strong-base AEM is defined as the ion exchange capacity (IEC) minus negative charges excluding OH^-, HCO_3^-, and CO_3^{2-}. The largest difference between a strong-base AEM and an aqueous solution is that the concentration of water in the sorbent is not large enough to be regarded as constant. The change of hydration status around counter ions that depends on the water loading in a strong-base AEM needs to be taken into consideration[3 4]. In a strong-base AEM, the chemical reactions that include hydration water attached to counter ions can be written as[4 23]:

$$\mathrm{CO}_{2(\mathrm{g})} \overset{K_{H(\mathrm{AEM})}}{\rightleftharpoons} \mathrm{CO}_{2(\mathrm{AEM})} \tag{33}$$

$$\mathrm{CO}_{2(\mathrm{AEM})} + \mathrm{OH}^-(\mathrm{H_2O})_{\mathrm{z}} \overset{K_{1(\mathrm{AEM})}}{\rightleftharpoons} \mathrm{HCO_3}^-(\mathrm{H_2O})_{\mathrm{x}} + n_1\mathrm{H_2O} \tag{34}$$

$$\mathrm{HCO_3}^-(\mathrm{H_2O})_{\mathrm{x}} + \mathrm{OH}^-(\mathrm{H_2O})_{\mathrm{z}} + n_2\mathrm{H_2O} \overset{K_{2(\mathrm{AEM})}}{\rightleftharpoons} \mathrm{CO_3}^{2-}(\mathrm{H_2O})_{\mathrm{y}} \tag{35}$$

where,

$$n_1 \equiv z - x \tag{36}$$

$$n_2 \equiv y - 1 - x - z \tag{37}$$

Note that x, y and z denotes the number of hydration H_2O molecules bounded to each counter ion, HCO_3^-, CO_3^{2-} and OH^-.

If we eliminate the $[OH^-]$ term, we obtain

$$2\,\mathrm{HCO_3}^-(\mathrm{H_2O})_{\mathrm{x}} + n\mathrm{H_2O} \rightleftharpoons \mathrm{CO_3}^{2-}(\mathrm{H_2O})_{\mathrm{y}} + \mathrm{CO_2} \tag{38}$$

where,

$$n \equiv n_1 + n_2 \tag{39}$$

$$= y - 2x - 1 \tag{40}$$

For the moisture-swing materials to satisfy the Le Châtelier-Braun principle[37], $y-2x-1$ has to be positive. Correspondingly, the equilibrium constants have to be updated according to the law of mass action[37 38] as

$$K_{1(\mathrm{AEM})} \equiv \frac{[\mathrm{HCO_3^-(H_2O)}_x][\mathrm{H_2O}]^{n_1}}{[\mathrm{CO_2}][\mathrm{OH^-(H_2O)}_z]} \tag{41}$$

$$K_{2(\mathrm{AEM})} \equiv \frac{[\mathrm{CO_3^{2-}(H_2O)}_y]}{[\mathrm{HCO_3^-(H_2O)}_x][\mathrm{OH^-(H_2O)}_z][\mathrm{H_2O}]^{n_2}} \tag{42}$$

Taking the update of the definition of the equilibrium constants from $[K_1, K_2]$ to $[K_{1(\mathrm{AEM})}, K_{2(\mathrm{AEM})}]$ into consideration, Eq.(28) is modified to:

$$\begin{aligned}\theta = {} & \frac{K_{\mathrm{H(AEM)}}K_{1\mathrm{(AEM)eff}}P_{\mathrm{CO_2}} - 1}{8K_{\mathrm{H(AEM)}}K_{1\mathrm{(AEM)eff}}K_{2\mathrm{(AEM)eff}}P_{\mathrm{CO_2}}[\mathrm{A}]} \\ & \times \{\sqrt{\eta} - (1 + K_{\mathrm{H(AEM)}}K_{1\mathrm{(AEM)eff}}P_{\mathrm{CO_2}})\} \\ & + \frac{1}{2}\end{aligned} \tag{43}$$

where,

$$\begin{aligned}\eta \equiv {} & (1 + K_{\mathrm{H(AEM)}}K_{1\mathrm{(AEM)eff}}P_{\mathrm{CO_2}})^2 \\ & + 8K_{\mathrm{H(AEM)}}K_{1\mathrm{(AEM)eff}}K_{2\mathrm{(AEM)eff}}P_{\mathrm{CO_2}}[\mathrm{A}]\end{aligned} \tag{44}$$

and

$$K_{1\mathrm{(AEM)eff}} \equiv K_{1\mathrm{(AEM)}} \times [\mathrm{H_2O}]^{-n_1} \tag{45}$$

$$K_{2\mathrm{(AEM)eff}} \equiv K_{2\mathrm{(AEM)}} \times [\mathrm{H_2O}]^{n_2} \tag{46}$$

Eq.(43) is the expression of θ for a strong-base AEM that corresponds to Eq.(28) for an alkali liquid. Eq.(43) indicates that, even if $K_{1(\mathrm{AEM})}$ and $K_{2(\mathrm{AEM})}$ are constant, the effective coefficients $K_{1(\mathrm{AEM})}$ and $K_{2(\mathrm{AEM})}$ (i.e. $K_{1\mathrm{(AEM)eff}}$ and $K_{2\mathrm{(AEM)eff}}$) change as function of $[H_2O]$ according to Eq.(45) and Eq.(46).

In the same way, Eq.(29) and Eq.(30) can be extended to:

$$\theta = \frac{K_{\mathrm{eq(AEM)}}[\mathrm{H_2O}]^{-n}P_{\mathrm{CO_2}}}{4}\left(\sqrt{1+\frac{4}{K_{\mathrm{eq(AEM)}}[\mathrm{H_2O}]^{-n}P_{\mathrm{CO_2}}}}-1\right) + \frac{1}{2} \tag{47}$$

$$= \frac{K_{\mathrm{eq(AEM)eff}}P_{\mathrm{CO_2}}}{4}\left(\sqrt{1+\frac{4}{K_{\mathrm{eq(AEM)eff}}P_{\mathrm{CO_2}}}}-1\right)+\frac{1}{2} \tag{48}$$

where,

$$K_{\mathrm{eq(AEM)}} \equiv \frac{K_{1\mathrm{(AEM)}}K_{\mathrm{H(AEM)}}}{2K_{2\mathrm{(AEM)}}[\mathrm{A}]} \tag{49}$$

$$K_{\mathrm{eq(AEM)eff}} \equiv K_{\mathrm{eq(AEM)}}[\mathrm{H_2O}]^{-n} \tag{50}$$

Eq.(48) is the expression of θ for a strong-base AEM that corresponds to Eq.(29) for an alkali liquid. Since this expression had been derived using the negligible $[\mathrm{CO_2}]$, $[\mathrm{H^+}]$ and $[\mathrm{OH^-}]$ approximation for an alkali liquid, we need to check if this approximation is still valid for a strong-base AEM in our Area of Interest.

Fig.(3) shows the comparison between S_{I} and S_{IV}, in which the equilibrium constant $K_{1\mathrm{(AEM)}}$ or $K_{2\mathrm{(AEM)}}$ are effectively changed to 100 and 5,000 times smaller or larger than the value in an aqueous solution at 25°C. This plot suggests that the negligible $[\mathrm{OH^-}]$ approximation is still valid in our Area of Interest (a few tens of Pascal for absorption and up to more than 10 kPa for desorption) even if $K_{1\mathrm{(AEM)eff}}$ or $K_{2\mathrm{(AEM)eff}}$ value is 100 times or even 5,000 times smaller or larger than K_1° or K_2°.

3 Result: Validation of the isotherm equation using literature data

In this section, we validate the theoretically derived isotherms using actual moisture-controlled $\mathrm{CO_2}$ sorption isotherm data that have been reported in prior research[3]. The digital data was obtained by digitizing the figures in the original paper. The value of θ was recalculated based on our definition of θ (see Eq.(22)) in this paper.

3.1 Isotherm data from a wet strong-base AEM

The isotherm data from a wet strong-base AEM sample are plotted in Fig.(4). If the isotherm follows a Langmuir-type model, the data points follow a straight line in a plot of $1/(2\theta-1)$ against $1/\mathrm{P_{CO_2}}$. The figure confirms that a Langmuir-type model is valid for larger $\mathrm{P_{CO_2}}$ values. The data start deviating from a straight line as $\mathrm{P_{CO_2}}$ gets smaller. We can observe that our newly derived equation for a moisture-controlled $\mathrm{CO_2}$ sorption isotherm, Eq.(48), can explain this nonlinearity in the data. The data fit quantitatively over the entire range in our Area of Interest at each temperature from 24°C to 45°C. The property of this sorbent in equilibrium can be represented by just a single parameter, $K_{\mathrm{eq(AEM)eff}}$. The ratio $K_{\mathrm{eq(AEM)eff}}/K^\circ_{\mathrm{eq}}$ is an indicator of how far the properties of a strong-base AEM deviate from that of an alkali liquid. The calculated values of $K_{\mathrm{eq(AEM)eff}}/K^\circ_{\mathrm{eq}}$ are sum-

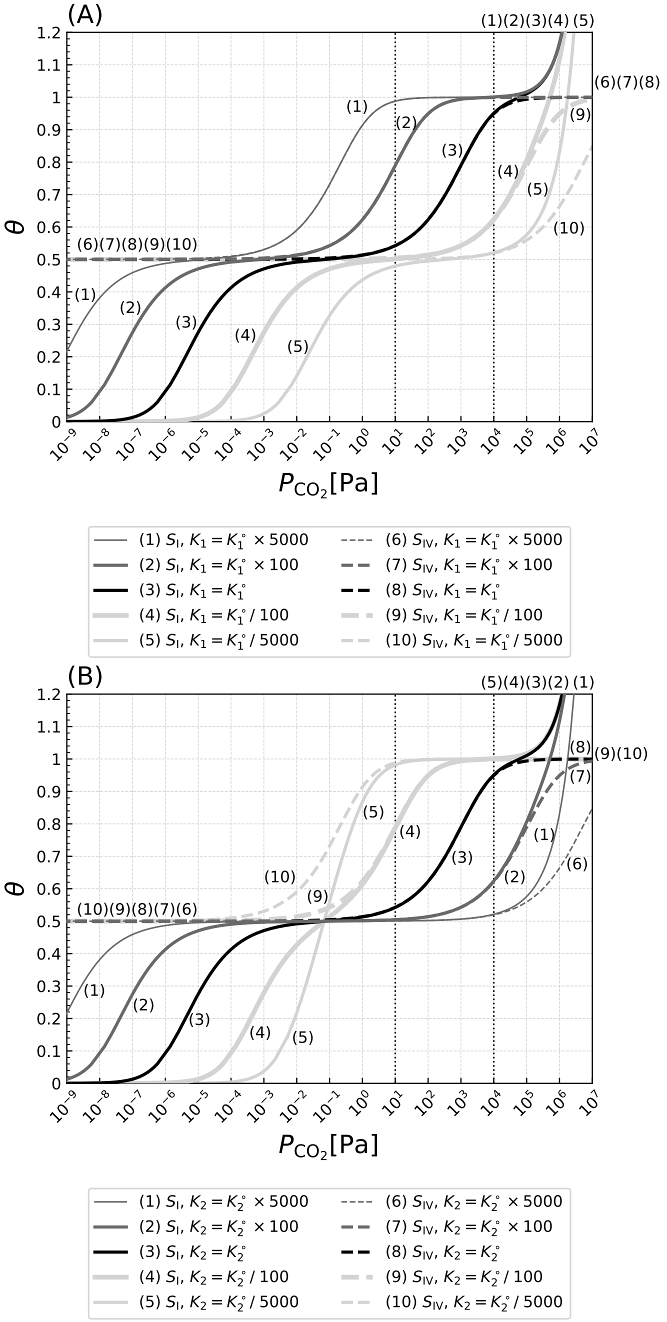

Fig. 3 Comparison between the exact isotherm equation (S_{I}) and the approximate isotherm valid for negligible $[\mathrm{CO_2}]$, $[\mathrm{H^+}]$ and $[\mathrm{OH^-}]$ (S_{IV}). [A] and temperature are assumed to be 2 mol $\mathrm{L^{-1}}$ and 25°C, respectively. The top figure (A) evaluates isotherms for different choices of K_1, 100 or 5000 times larger or smaller than K_1°. The bottom figure (B) instead varies K_2. The other parameters are assumed to be unchanged from those in an alkali liquid. I.e., $K_W = K_W^\circ$, $K_H = K_H^\circ$, $K_2 = K_2^\circ$ (A) or $K_1 = K_1^\circ$ (B). The vertical lines in (A) and (B) indicate the range of our Area of Interest.

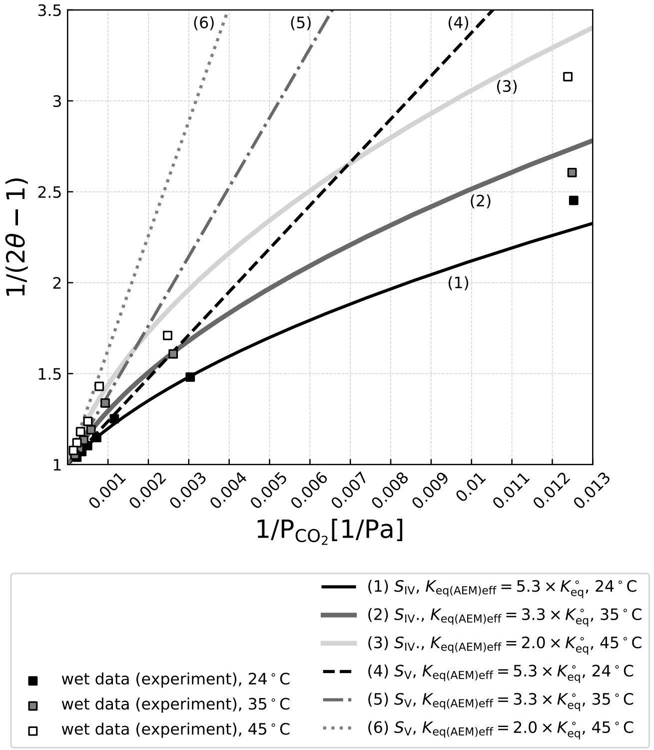

Fig. 4 The comparison between S_{IV} (Eq.(48)) and experimental moisture-controlled CO_2 sorption isotherm data of a wet strong-base AEM that has been reported in the literature[3].

marized in Table(1). Note that the [IEC] of this strong-base AEM is 1.90 mmol g^{-1}[3]. Table(1) shows that the value of $K_{\mathrm{eq(AEM)eff}}$ in a wet strong-base AEM is slightly higher than K°_{eq} for an alkali liquid but of the same order of magnitude. The deviation from an alkali liquid significantly increases as the strong-base AEM loses water, which causes moisture-controlled CO_2 sorption, according to Eq.(48).

Table 1 Summary of the calculated $K_{\mathrm{eq(AEM)eff}}/K^{\circ}_{\mathrm{eq}}$ values.

sample	temperature [° C]	$K_{\mathrm{eq(AEM)eff}}/K^{\circ}_{\mathrm{eq}}$
alkali liquid	25	1 (by definition)
strong-base AEM (wet)	45	2.0
strong-base AEM (wet)	35	3.3
strong-base AEM (wet)	24	5.3
strong-base AEM (dry)	23	3400

3.2 Isotherm data from a dry strong-base AEM

The isotherm data from a dry strong-base AEM sample are plotted in Fig.(5) and fitted using Eq.(48) with $K_{\mathrm{eq(AEM)eff}} = 3400K^{\circ}_{\mathrm{eq}}$. Since this value is significantly higher compared to that in a wet strong-base AEM, Eq.(48) is closer to a Langmuir-type model. Indeed, we can observe that the data distribution shows less non-linearity in Fig.(5).

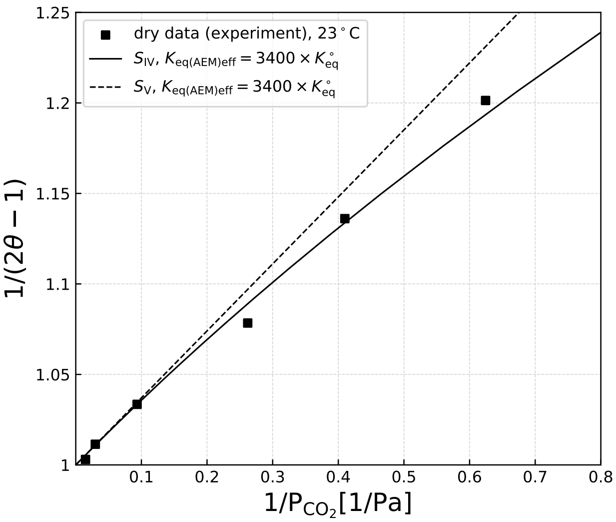

Fig. 5 The comparison between S_{IV} (Eq.(48)) and experimental moisture-controlled CO_2 sorption isotherm data of a dry strong-base AEM that has been reported in the literature[3].

4 Discussion: Physical interpretation of the isotherm equations for strong-base AEMs

4.1 The driving force of moisture-controlled CO_2 sorption

Wang et al.[4] pointed out that the Langmuir constant of moisture-controlled CO_2 sorption in a strong-base AEM changes by a factor of roughly 500 as the relative humidity is varied from 20% to 100%. The Langmuir constant was obtained by fitting empirically the experimental isotherm data to a Langmuir-type model. We derived this Langmuir constant as $K_{\mathrm{eq(AEM)eff}} = \frac{K_{1(\mathrm{AEM})}K_{\mathrm{H(AEM)}}}{2K_{2(\mathrm{AEM})}[\mathrm{A}]}[\mathrm{H_2O}]^{-n} = K_{\mathrm{eq(AEM)}}[\mathrm{H_2O}]^{-n}$ based on the governing equations. Therefore moisture-controlled CO_2 sorption can be explained even if the equilibrium constants of the chemical reactions ($K_{1(\mathrm{AEM})}$,$K_{2(\mathrm{AEM})}$ and $K_{\mathrm{eq(AEM)}}$) are constant. Instead, the additional factor $[\mathrm{H_2O}]^{-n}$ transforms $K_{\mathrm{eq(AEM)}}$ into $K_{\mathrm{eq(AEM)eff}}$, which indeed depends on humidity. A wet environment (resulting in a small $[\mathrm{H_2O}]^{-n}$ term) causes $K_{\mathrm{eq(AEM)eff}}$ to be small but keeps the original $K_{\mathrm{eq(AEM)}}$ constant. This formulation agrees with the Le Châtelier-Braun principle[37]. According to this, the chemical reaction Eq.(38) is driven to the right-hand side (namely, to emit CO_2) when $[\mathrm{H_2O}]$ is larger (namely, wet).

4.2 Indistinguishability of $K_{1(\mathrm{AEM})\mathrm{eff}}$ and $K_{2(\mathrm{AEM})\mathrm{eff}}$

Eq.(45), Eq.(46) and Eq.(43) indicate that $K_{1(\mathrm{AEM})\mathrm{eff}}$ and $K_{2(\mathrm{AEM})\mathrm{eff}}$ are affected by different $[\mathrm{H_2O}]$ terms independently. Both can contribute to the change of the equilibrium CO_2 partial pressure over a strong-base AEM. However, Eq.(48) shows that $K_{1(\mathrm{AEM})}$ and $K_{2(\mathrm{AEM})}$ appear as $\frac{K_{1(\mathrm{AEM})}}{K_{2(\mathrm{AEM})}}$ when the approximation for S_{IV} is valid. In this case, one cannot tell whether the change of the isotherm comes from changes in $K_{1(\mathrm{AEM})\mathrm{eff}}$ or $K_{2(\mathrm{AEM})\mathrm{eff}}$ by just observing the isotherm data. We define an indicator of distinguishability between $K_{1(\mathrm{AEM})\mathrm{eff}}$ and $K_{2(\mathrm{AEM})\mathrm{eff}}$ as

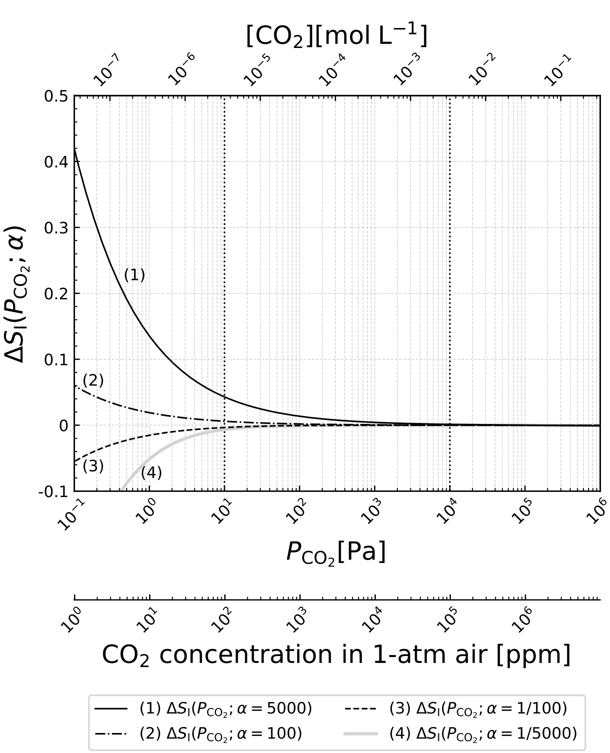

Fig. 6 The plot of $\Delta S_I(P_{CO_2};\alpha)$ with $\alpha = 5000^{-1}$, 100^{-1}, 100 or 5000. Note that all the x-axes use logarithmic scales. The vertical lines indicate the range of our Area of Interest.

$$\Delta S_I(P_{CO_2};\alpha) \quad \equiv \quad \frac{S_{I\alpha}(P_{CO_2};1,\alpha) - S_{I\alpha}(P_{CO_2};\alpha^{-1},1)}{\{S_{I\alpha}(P_{CO_2};1,\alpha) + S_{I\alpha}(P_{CO_2};\alpha^{-1},1)\}/2} \tag{51}$$

where,

$$S_{I\alpha}(P_{CO_2};\alpha_1,\alpha_2) \quad \equiv \quad S_I(P_{CO_2};K_1 = \alpha_1 K_1^\circ, K_2 = \alpha_2 K_2^\circ, K_H = K_H^\circ) \tag{52}$$

If we define $S_{IV\alpha}$ and ΔS_{IV} in the same way, ΔS_{IV} is always zero regardless of the value of α, which means $K_{1(AEM)eff}$ and $K_{2(AEM)eff}$ are indistinguishable. However, when the approximation for S_{IV} is not good enough, ΔS_I can have a non-zero value. Fig.(6) shows ΔS_I with $\alpha = 5000^{-1}$, 100^{-1}, 100 and 5000. In our Area of Interest, ΔS_I takes the maximum values at the lower P_{CO_2} due to the larger $[OH^-]$. Even in an extreme case of $\alpha = 5000$, the difference between S_I and S_{IV} is 4.3% at its maximum. For the other values of α, the maximum differences range from 0.35% to 0.65%. It would take extreme measurement accuracy to differentiate between changes in $K_{2(AEM)eff}$ or $K_{1(AEM)eff}$.

4.3 Physical meaning of $K_{eq(AEM)eff}/K_{eq}^\circ$

We have generalized the theory of an alkali liquid to a strong-base AEM and treat them in a unified way. The non-dimensional parameter $K_{eq(AEM)eff}/K_{eq}^\circ$ characterizes an isotherm of strong-base AEMs in a quantitative way, taking values from 1 to $\sim$ 3400. $K_{eq(AEM)eff}/K_{eq}^\circ$ is defined as 1 for an alkali liquid at 25°C and can be regarded as an indicator of how the property of a strong-base AEM deviates from that of an alkali liquid as the surrounding humidity level changes. For example, the value of a particular wet strong-base AEM turns out to be slightly higher than 1, but of the same order of magnitude ($K_{eq(AEM)eff}/K_{eq}^\circ = 1 \sim 10$). As the strong-base AEM sample dries out, $K_{eq(AEM)eff}/K_{eq}^\circ$ increases getting as large as $\sim$3400.

5 Conclusions

We have shown that the governing equations of the moisture-controlled CO$_2$ sorption can be reduced into a simple analytic isotherm equation by taking advantages of realistic approximations in our Area of Interest. The theory has been established for an alkali liquid first, then extended to strong-base AEMs. The final formula (Eq.(48)) contains only a single parameter, which means that the static properties of moisture-controlled CO$_2$ sorbents can be characterized by just one parameter $K_{eq(AEM)eff}$. This parameter can be decomposed into two terms as $K_{eq(AEM)eff} = K_{eq(AEM)} \times [H_2O]^{-n}$. The first factor $K_{eq(AEM)}$ combines all the independent material-specific parameters such as [A], K_H, K_1 and K_2, which are indistinguishable in isotherm data. The second factor $[H_2O]^{-n}$ accounts for the fact that humidity level changes the CO$_2$ affinity of the sorbent. Overall, we suggest that the equilibrium constant of the chemical reactions inside strong-base AEMs is effectively changed from $K_{eq(AEM)}$ to $K_{eq(AEM)}[H_2O]^{-n}$ due to changes in humidity.

It has been demonstrated that the final equation (Eq.(48)) fits well to the actual isotherm data of both a wet and dry strong-base AEM that have been reported in the literature[3]. By comparison to the existing data, the difference between a site balance equation like the Langmuir equation and our more complex model matters and is clearly visible in the data. The equation provides the appropriate correction to the systematic misfit between a Langmuir-type model and the isotherm data that occurs especially at lower values of P_{CO_2} within our Area of Interest. The concept of $K_{eq(AEM)eff}/K_{eq}^\circ$ has been introduced to bridge the theory for an alkali liquid to that for a strong-base AEM seamlessly. $K_{eq(AEM)eff}/K_{eq}^\circ$ is a unique parameter that by itself can characterize the property of the sorbents in equilibrium. $K_{eq(AEM)eff}/K_{eq}^\circ$ increases to $\sim$ 3400 as a strong-base AEM loses water. The value gets smaller as the sorbents take up water, which causes a change in the equilibrium pressure of CO$_2$ over the sorbent according to Eq.(48). $K_{eq(AEM)eff}/K_{eq}^\circ$ is defined so that it takes the value of 1 for an ideal alkali liquid at 25°C, so $K_{eq(AEM)eff}/K_{eq}^\circ$ can be also regarded as an indicator that shows how far the property of strong-base AEM deviates from that of an alkali liquid.

Author Contributions

Yuta Kaneko: Conceptualization, Investigation, Methodology, Visualization, Writing (original draft)
Klaus S. Lackner: Supervision, Validation, Writing (review & editing)

Conflicts of Interest

Klaus S. Lackner is a coinventor of IP owned by Arizona State University (ASU) that relates to certain implementations of direct air capture. Lackner also consults for companies that work on direct air capture. ASU has licensed part of its IP to Carbon Collect and owns a stake in the company. As an employee of the University, Lackner is a technical advisor to the company and in recognition also received shares from the company. Carbon Collect also supports DAC research at ASU.

Acknowledgements

This research has been performed as a part of the Mining Air for Fuels and Fine Chemicals (MAFF) project led by Arizona State University, together with Northern Arizona University and The University of Texas at Austin. The authors acknowledge insightful discussions with Dr. Justin Flory, Dr. Jennifer Lynn Wade, Dr. Matthew D. Green, Dr. Benny D. Freeman, Dr. Kristofer L. Gleason, Hoda Shokrollahzadeh Behbahani, Husain Mithaiwala, Horacio Lopez Marques and Winston Wang. The authors are also grateful for the support from the Center for Negative Carbon Emissions (CNCE) at Arizona State University.

The information, data, or work presented herein was funded in part by the Advanced Research Projects Agency-Energy (ARPA-E), U.S. Department of Energy, under Award Number DE-AR0001103. The views and opinions of authors expressed herein do not necessarily state or reflect those of the United States Government or any agency thereof.

Notes and references

1 K. Lackner, *The European physical journal. ST, Special topics*, 2009, **176**, 93–106.

2 K. S. Lackner and S. Brennan, *Climatic change*, 2009, **96**, 357–378.

3 T. Wang, K. S. Lackner and A. Wright, *Environmental science & technology*, 2011, **45**, 6670–6675.

4 T. Wang, K. S. Lackner and A. B. Wright, *Physical Chemistry Chemical Physics*, 2012, **15**, 504–514.

5 K. Lackner, H.-J. Ziock and P. Grimes, Conference: 24th Annual Technical Conference on Coal Utilization and Fuel Systems, Clearwater, 1999a.

6 K. Lackner, P. Grimes and H. Ziock, *Carbon dioxide extraction from air? Los Alamos National Laboratory*, LAUR-99-5113, Los Alamos, NM technical report, 1999b.

7 D. W. Keith, M. Ha-Duong and J. K. Stolaroff, *Climatic change*, 2006, **74**, 17–45.

8 K. S. Lackner, in *Geoengineering of the climate system*, Royal Society of Chemistry, 2014, vol. 38, ch. The use of artificial trees, p. 80.

9 E. S. Sanz-Pérez, C. R. Murdock, S. A. Didas and C. W. Jones, *Chemical reviews*, 2016, **116**, 11840–11876.

10 European Academies' Science Advisory Council (EASAC), *Negative emission technologies: What role in meeting Paris Agreement targets?*, European academies' science advisory council (easac) technical report, 2018.

11 D. W. Keith, *Science (American Association for the Advancement of Science)*, 2009, **325**, 1654–1655.

12 K. S. Lackner, S. Brennan, J. M. Matter, A.-H. A. Park, A. Wright and B. van der Zwaan, *Proceedings of the National Academy of Sciences - PNAS*, 2012, **109**, 13156–13162.

13 V. Masson-Delmotte, P. Zhai, A. Pirani, S. L. Connors, C. Péan, S. Berger, N. Caud, Y. Chen, L. Goldfarb, M. I. Gomis, M. Huang, K. Leitzell, E. Lonnoy, J. B. R. Matthews, T. Maycock, T. Waterfield, O. Yelekçi, R. Yu and B. Zhou(eds.), *Cambridge University Press*, 2021.

14 American Physical Society, *Direct Air Capture of CO_2 with Chemicals: A Technology Assessment for the APS Panel on Public Affairs*, American physical society technical report, 2011.

15 National Academies of Sciences, Engineering, and Medicine., *Negative Emissions Technologies and Reliable Sequestration: A Research Agenda.*, Washington, DC: The National Academies Press., 2019.

16 K. S. Lackner and H. Azarabadi, *Industrial & engineering chemistry research*, 2021, **60**, 8196–8208.

17 J. A. Wurzbacher, C. Gebald and A. Steinfeld, *Energy and Environmental Science*, 2011, **4**, 3584–3592.

18 D. W. Keith, G. Holmes, D. S. Angelo and K. Heidel, *Joule*, 2018, **2**, 2197.

19 K. Foo and B. Hameed, *Chemical engineering journal (Lausanne, Switzerland : 1996)*, 2010, **156**, 2–10.

20 C. Hou, D. R. Kumar, Y. Jin, Y. Wu, J. J. Lee, C. W. Jones and T. Wang, *Chemical engineering journal (Lausanne, Switzerland : 1996)*, 2021, **413**, 127532–.

21 H. Xiao, X. Shi, Y. Zhang, X. Liao, F. Hao, K. S. Lackner and X. Chen, *Physical chemistry chemical physics : PCCP*, 2017, **19**, 27435–27441.

22 X. Wang, J. Song, Y. Chen, H. Xiao, X. Shi, Y. Liu, L. Zhu, Y.-L. He and X. Chen, *Industrial & engineering chemistry research*, 2020, **59**, 16507–16515.

23 X. Shi, H. Xiao, K. Kanamori, A. Yonezu, K. S. Lackner and X. Chen, *Joule*, 2020, **4**, 1823–1837.

24 G. Sposito, *The surface chemistry of soils*, Oxford University Press, New York, 1984.

25 P. Van Cappellen, L. Charlet, W. Stumm and P. Wersin, *Geochimica et Cosmochimica Acta*, 1993, **57**, 3505–3518.

26 C. R. Harte, E. M. Baker and H. H. Purcell, *Industrial and engineering chemistry*, 1933, **25**, 528–531.

27 J. N. Butler, *Carbon dioxide equilibria and their applications*, Addison-Wesley, Reading, Mass, 1982.

28 D. M. Kern, *Journal of chemical education*, 1960, **37**, 14–.

29 H. Hikita, S. Asai and T. Takatsuka, *The Chemical Engineering Journal*, 1976, **11**, 131–141.

30 W. A. House, J. R. Howard and G. Skirrow, *Faraday Discuss. Chem. Soc.*, 1984, **77**, 33–46.

31 H. S. Harned and R. Davis, *Journal of the American Chemical Society*, 1943, **65**, 2030–2037.

32 H. S. Harned and S. R. Scholes, *Journal of the American Chemical Society*, 1941, **63**, 1706–1709.

33 F. J. Millero, *Geochimica et Cosmochimica Acta*, 1995, **59**, 661–677.

34 W. G. Mook, *Environmental isotopes in the hydrological cycle: principles and applications, v. I: Introduction; theory, methods, review*, 2000.

35 I. Rémy, *Numerical Simulation of a Carbon Dioxide Pump*, École Polytechnique Université Paris-Saclay technical report, 2014.

36 A. Robin, *Modelisation and Calibration of moisture sensitive beads in Carbon dioxide capture*, École Polytechnique Université Paris-Saclay technical report, 2015.

37 A. Bejan, *Advanced Engineering Thermodynamics*, John Wiley & Sons, Incorporated, Newark, 2016.

38 J. K. Baird, *Journal of chemical education*, 1999, **76**, 1146–.